

NPS ARCHIVE  
1960  
COTTRELL, W.

A DETERMINATION OF THE COEFFICIENT  
OF EDDY CONDUCTIVITY FROM  
MICROMETEOROLOGICAL PARAMETERS

WALTER N. COTTRELL

Library  
U. S. Naval Postgraduate School  
Monterey, California









A DETERMINATION OF THE COEFFICIENT  
OF EDDY CONDUCTIVITY FROM  
MICROMETEOROLOGICAL PARAMETERS

\* \* \* \* \*

Walter N. Cottrell





A DETERMINATION OF THE COEFFICIENT  
OF EDDY CONDUCTIVITY FROM  
MICROMETEOROLOGICAL PARAMETERS

by

Walter N. Cottrell  
//

Lieutenant, United States Navy

Submitted in partial fulfillment of  
the requirements for the degree of

MASTER OF SCIENCE  
IN  
METEOROLOGY

United States Naval Postgraduate School  
Monterey, California

1 9 6 0

NYS ARCHIVE

960

COTTRELL, W.

Thesis  
27564

A DETERMINATION OF THE COEFFICIENT  
OF EDDY CONDUCTIVITY FROM  
MICROMETEOROLOGICAL PARAMETERS

\* \* \* \* \*

Walter N. Cottrell

1 9 6 0

UNITED STATES NAVAL POSTGRADUATE SCHOOL

Degree: Master of Science in  
Meteorology

Classification:

Thesis: Unclassified

Abstract: Unclassified

Title of Thesis: Unclassified

Contains no proprietary information.



A DETERMINATION OF THE COEFFICIENT  
OF EDDY CONDUCTIVITY FROM  
MICROMETEOROLOGICAL PARAMETERS

by

Walter N. Cottrell

This work is accepted as fulfilling  
the thesis requirements for the degree of

MASTER OF SCIENCE

IN

METEOROLOGY

from the

United States Naval Postgraduate School



## ACKNOWLEDGEMENT

The author is deeply indebted to Professor Frank L. Martin for his advice and guidance during the progress of the investigation. Appreciation is expressed to the author's wife, Carolyn Cottrell, for her inspiration and aid in making some of the computations and for her part in typing the rough draft of the paper. Grateful acknowledgement is also due Lt. Kenneth Ruggles for the use of his excellent statistics routine for the NCR 102A electronic digital computer.





## ABSTRACT

Considering the absorption of terrestrial radiation by carbon dioxide and water vapor, coefficients of eddy conductivity are computed for heights in the range 4 to 320 meters from data collected during the Great Plains Field Program (August and September 1953.) Power-law profiles with height are fitted to the computed coefficients and values obtained from the fitted profiles correlated with a stability parameter.



## TABLE OF CONTENTS

Section	Title	Page
1.	Introduction	1
2.	The Great Plains data	3
2.1	Instrumental errors	5
3.	Background, methods, and equations	7
3.1	The water vapor problem	9
3.2	The carbon dioxide radiation problem	12
4.	Computations	18
4.1	The water vapor radiative temperature change	18
4.2	The radiative temperature change due to carbon dioxide	20
4.3	The local rate of change of temperature	21
4.4	Advective temperature changes	24
4.5	The coefficient of eddy conductivity	26
5.	Results	31
5.1	$\bar{K}_H$ as a function of height	31
5.2	$\bar{K}_H$ as a function of stability	39
6.	Conclusions	40
7.	Bibliography	42



## LIST OF TABLES

Table		Page
1.	Infrared radiative temperature change ( $^{\circ}\text{C}/\text{Hr}$ ) due to water vapor	19
2.	Infrared radiative temperature change ( $^{\circ}\text{C}/\text{Hr}$ ) due to carbon dioxide	20
3.	Average local rate of change of temperature ( $^{\circ}\text{C}/\text{Hr}$ )	23
4.	Average lapse rate of potential temperature ( $^{\circ}\text{C}/\text{meter}$ )	27
5.	Computed values of $\bar{K}_H$ ( $\text{cm}^2/\text{sec}$ )	30
6.	$\bar{K}_H$ as an exponential function of height	31
7.	Linear correlation coefficients of $\Delta\Theta$ with $\bar{K}_H$ and $\Delta\Theta$ with m	39



## LIST OF ILLUSTRATIONS

Figure		Page
1.	Scatter of micrometeorological temperature observations for the 0635 sounding	6
2.	Percent absorption of terrestrial radiation due to CO <sub>2</sub> in the 12.2 - 17.5 $\mu$ band (after Brooks)	16
3.	L-20 temperature sounding (centered at 1235 CST)	22
4.	Hodograph of the geostrophic wind for 7 September-0900 (values are estimated for the O'Neill site from local synoptic charts.)	25
5.	$\bar{K}_H$ as a function of height for the 0735 sounding	32
6.	$\bar{K}_H$ as a function of height for the 0935 sounding (without advection)	33
7.	$\bar{K}_H$ as a function of height for the 0935 sounding (with advection)	34
8.	$\bar{K}_H$ as a function of height for the 1135 sounding	35
9.	$\bar{K}_H$ as a function of height for the 1335 sounding	35
10.	$\bar{K}_H$ as a function of height for the 1535 sounding	37





## LIST OF ABBREVIATIONS AND SYMBOLS

$C_p$	specific heat of air at constant pressure
CST	Central Standard Time
$f$	Coriolis parameter
$g$	acceleration of gravity
JH	Johns Hopkins University
log	logarithm to the base 10
MIT	Massachusetts Institute of Technology
OBS	observed
RAD	radiative change of temperature
$R_d$	gas constant for dry air
$T$	temperature
TURB	turbulent change
UCLA	University of California at Los Angeles
UT	University of Texas
WV	water vapor
$z$	height measured from the ground
$\epsilon_f$	flux-emissivity
$\delta_d$	dry adiabatic lapse rate ( $0.98^\circ\text{C}/100$ meters)
$\rho$	air density
$\sigma$	Stefan-Boltzman constant
$\tau_f$	flux-transmissivity
$\theta$	potential temperature



## 1. Introduction.

An important step forward in the theory of the turbulent transfer of properties in the lower layers of the atmosphere was taken when the concept of Austauschkoefizienten or "exchange coefficients" was proposed by Wilhelm Schmidt in 1925. Since that time several attempts have been made by various workers to measure these coefficients through experimental observations in order to test the theory of turbulent exchange. In 1950 Cooley [5] made determinations of eddy conductivity near the earth's surface from data gathered at Manor, Texas. About the same time Jehn and Gerhardt [9] made measurements of eddy heat flux up to about 120 meters at Manor and Gila Bend, Arizona. In addition to these were the observations of Cramer and Record [6] near the earth's surface in 1953, and a small number of observations due to other workers in the period 1955-1957. These observations have been summarized by Priestly [11], and no attempt will be made here to review all of the results.

The primary reason that the number of such observations has been small is that the accurate determination of micrometeorological parameters is exceedingly difficult and very expensive. For this reason the quality and volume of such data obtained in the past have been far below the level of desirability.

The publication of the "Proceedings of the Great Plains Turbulence Field Program, 1 August to 8 September 1953, O'Neill, Nebraska" made new and better data available for the study of the turbulent transport of properties in the atmosphere's lowest layers. In order to obtain new



evidence on the nature of the turbulent heat and momentum transports and their relationships to one another, it was originally decided to initiate thesis projects at the United States Naval Postgraduate School. These projects to be undertaken were to determine the coefficients of (1) eddy conductivity,  $K_H$ , (2) eddy viscosity,  $K_M$ , and (3) the ratio of the two coefficients,  $K_H/K_M$  from this new micrometeorological data. In particular this present study involves the determination of the coefficient of eddy conductivity and the examination of its variation with height and stability from the values determined.



## 2. The Great Plains data.

The data collection program for the Great Plains project was broken down into seven time-observation periods with a multitude of parameters being observed at nearly equally spaced observation times within each period.

For this study the seventh observation period (7 and 8 September) was used and was considered to be the most suitable of the periods on the basis of a combination of two factors; (1) completeness of data utilized in the study and (2) a minimum of advection during the period. As an aid in the interpretation of the results the following quotation  $\overline{10}$  is provided concerning the synoptic conditions in the area during the seventh period:

On 7 September, the high-pressure area east of Nebraska moved eastward while a trough of low pressure approached from the west. The winds were southerly and initially light, becoming 15 to 20 mph. The skies were generally clear over Nebraska with some scattered cirrus during the morning of the 8th. Cumulonimbus clouds and lightning were visible to the north of the test site from the afternoon of the 7th, until the early morning of the 8th. The seventh and last general observation period began at 0405 CST on 7 September and continued until 1305 CST on 8 September under relatively favorable conditions.

Of the many tables of data included in  $\overline{10}$ , the following summary shows those which were used in this study:

<u>Table number</u> <sup>1</sup>	<u>Data used</u> <sup>2</sup>
1.1a	7 September, 1900, CST, West and South components of the geostrophic wind at indicated pressure levels. Values estimated from local synoptic charts.

<sup>1</sup>Table where numbers of the form 1.1 etc., refer to tables in  $\overline{10}$

<sup>2</sup>Where times are omitted, data were available for each sounding





Table Number<sup>1</sup>Data Used<sup>2</sup>

1.3	Station pressure and relative humidity
2.1a	Soil temperature at 0.5 cm below the surface of the ground (taken as being representative of the ground temperature.)
4.2	Mean air temperature from aspirated thermocouples (MIT, 15-minute means at 2.0, 4.0, 8.0 and 16.0 meters above the ground, UCLA, average of six readings taken every 3 minutes at various levels up to 8.0 meters); shielded thermocouples (JH, average of 20 readings at each level during a 5-minute interval at various levels up to 6.4 meters) and shielded thermistors (UT, 10-second means at various levels up to .8 meters.)
5.2a	Mean cross product of vertical eddy velocity component and air temperature multiplied by density and specific heat of air for 3.0, 6.0 and 12.0 meters above the ground. Values missing for 1235 and 1435.
6.4	Radiosonde pressure, temperature and relative humidity at significant levels.
6.5	Air temperature and mixing ratio at altitudes from aerograph (L-20) data. Time at start, top level and end of flight is indicated.
7.3a	Sensible heat transfer to the air from the earth-air interface according to theoretical models of Suomi and Lettau.

During the observation period, data were recorded bi-hourly for even hours of average local time (CST plus 35 minutes). Sufficient time and data were available to make  $K_H$  computations for six soundings, 0535, 0835, 1035, 1235, 1435 and 1635 on 7 September. Since no night-time aerograph observations were made, only daytime determinations were possible.



## 2.1. Instrumental errors .

Contributors to the Great Plains project have given the following values for instrumental errors inherent in the data:

1. Micrometeorological absolute temperature errors (Table 4.2)<sup>1</sup>
  - a) 0.2°C (UT)
  - b) 0.1°C (MIT and UCLA)
  - c) 0.05°C (JH)
  
2. The L-20 aerograph configuration<sup>2</sup> temperature and relative humidity errors.
  - a) Temperature error:
    - (1) 1°C absolute, for any level.
    - (2) Relative error between levels, 0.1°C.
  
  - b) Relative humidity error:
    - (1) to 10% absolute.
    - (2) Relative error between levels, 3%.

In 29 cases a comparison of MIT temperature values at 16.0 meters to the L-20 data at 17 meters gave a mean difference, MIT minus L-20 of  $-0.10 \pm 0.11^{\circ}\text{C}$ .

For a complete picture of the instrumentation, analysis of instrumental errors and a description of the test-site the reader is referred to

/10/.

<sup>1</sup>For an interesting comparison of observed micrometeorological temperatures see fig. 1.

<sup>2</sup>The L-20 configuration utilizes the KS-4 Kollsman aerograph, which is an automatic device for the automatic recording of temperature and relative humidity.



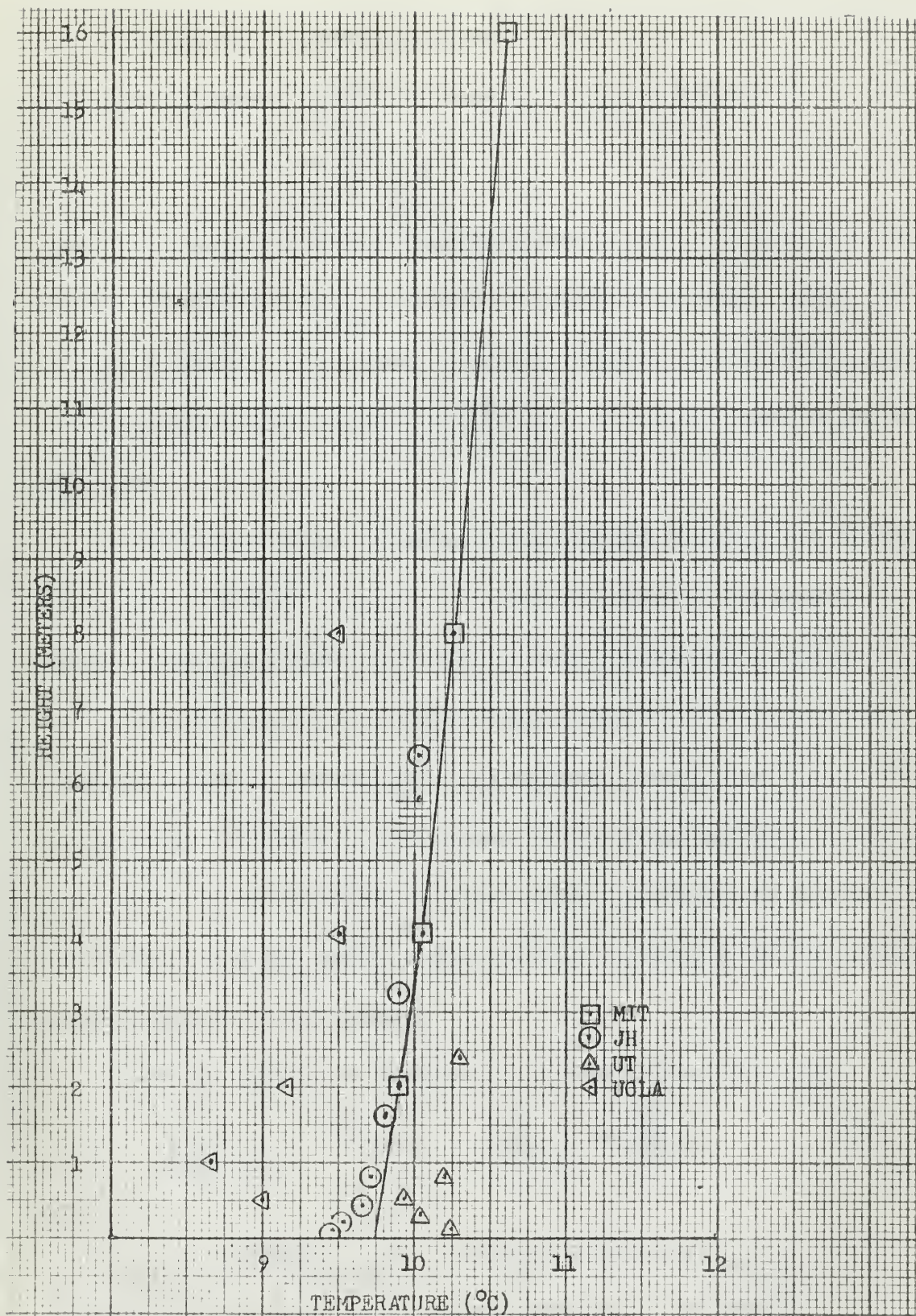


Fig. 1. Scatter of micrometeorological temperature observations for the 0035 sounding.



### 3. Background, methods and equations.

The coefficient of eddy conductivity,  $K_H$ , is defined by:

$$K_H = - \frac{Q}{\rho C_p \frac{d\bar{\theta}}{dz}} \quad (1)$$

where  $Q$  is the turbulent heat transfer in the vertical. It may be observed from this definition that  $K_H$  is always a positive quantity. When  $\frac{d\bar{\theta}}{dz}$  is negative (unstable conditions),  $Q$  will be positive and directed upward. Conversely for stable conditions ( $\frac{d\bar{\theta}}{dz} > 0$ ),  $Q$  will be negative and directed downward.

In this study starting values of  $K_H$  at 4 and 8 meters are computed by using eq. (1) with  $Q$  given by the average value in the layer 3-12 meters. For values above the starting level the following method is utilized.

The horizontal turbulent exchange of heat is usually very small compared to that in the vertical, and vertical advection is usually considered to be negligible in comparison to horizontal advection. The fact that clouds did not occur in the layer under study rules out a latent heat contribution, and the small height-variation of density can be overlooked for the layers to be considered.

Then the equation of turbulent diffusion for heat becomes:

$$\left(\frac{\partial \bar{\theta}}{\partial t}\right)_{TURB} = - \bar{v} \cdot \nabla_H \bar{\theta} + \frac{\partial}{\partial z} \left( K_H \frac{\partial \bar{\theta}}{\partial z} \right) \quad (2)$$

Also

$$\left(\frac{\partial \theta}{\partial t}\right)_{TURB} = \frac{\partial \theta}{\partial t} - \left(\frac{\partial \theta}{\partial t}\right)_{RAD}$$

Close to the ground the following approximations are valid:<sup>1</sup>

$$\frac{\partial \theta}{\partial t} \doteq \frac{\partial T}{\partial t}; \quad \frac{\partial \theta}{\partial z} \doteq \frac{\partial T}{\partial z} + \alpha_d; \quad - \bar{v} \cdot \nabla_H \theta = - \bar{v} \cdot \nabla_H T \quad (3)$$

<sup>1</sup> Hereinafter the bars over  $\theta$  and  $T$  will be omitted but understood.

The coefficient of eddy conductivity,  $K_H$ , is defined by

$$Q = -K_H \frac{\partial \theta}{\partial z}$$

where  $Q$  is the turbulent heat transfer in the vertical. It may be observed

from this definition that  $K_H$  is always a positive quantity. When  $Q$  is

negative (unstable conditions),  $Q$  will be positive and directed upward.

Conversely for stable conditions ( $\frac{\partial \theta}{\partial z} > 0$ ),  $Q$  will be negative and directed

downward.

In this study starting values of  $K_H$  at 4 and 8 meters are computed

by using eq. (1) with  $Q$  given by the average value in the layer 0-4

meters. For values above the starting level the following method is utilized.

The horizontal turbulent exchange of heat is usually very small

compared to that in the vertical, and vertical advection is usually non-

considered to be negligible in comparison to horizontal advection. The fact

that clouds did not occur in the layer under study rules out a latent heat

contribution, and the small height-variation of density can be overlooked

for the layers to be considered.

Then the equation of turbulent diffusion for heat becomes

$$\frac{\partial Q}{\partial z} = \frac{\partial}{\partial z} \left( -K_H \frac{\partial \theta}{\partial z} \right) = -\frac{\partial}{\partial z} \left( K_H \frac{\partial \theta}{\partial z} \right)$$

also

$$\frac{\partial Q}{\partial z} = -\frac{\partial}{\partial z} \left( K_H \frac{\partial \theta}{\partial z} \right)$$

Close to the ground the following approximations are valid:

$$\frac{\partial \theta}{\partial z} = \frac{\partial \theta}{\partial z} = -\frac{\partial \theta}{\partial z} = -\frac{\partial \theta}{\partial z}$$

Hereafter the bars over  $\theta$  and  $T$  will be omitted but understood.



Now returning to eq. (2) and substituting eq. (3) we get:

$$\frac{\partial T}{\partial t} = -\bar{V} \cdot \nabla_H T + \left( \frac{\partial T}{\partial t} \right)_{RAD} + \frac{\partial}{\partial z} \left( K_H \left( \frac{\partial T}{\partial z} + \gamma_d \right) \right) \quad (4)$$

In finite difference form this becomes:

$$\frac{\Delta T}{\Delta t} = \frac{K_2 \left( \frac{\Delta T}{\Delta z} + \gamma_d \right)_2 - K_1 \left( \frac{\Delta T}{\Delta z} + \gamma_d \right)_1}{\Delta z_{1-2}} - \bar{V} \cdot \nabla_H T + \left( \frac{\Delta T}{\Delta t} \right)_{RAD} \quad (5)$$

Transposing terms and solving for  $K_2$  gives:

$$K_2 = \frac{\left[ \left( \frac{\Delta T}{\Delta t} \right)_{OBS} + \bar{V} \cdot \nabla_H T - \left( \frac{\Delta T}{\Delta t} \right)_{RAD} \right] \Delta z_{1-2} + K_1 \left( \frac{\Delta T}{\Delta z} + \gamma_d \right)_1}{\left( \frac{\Delta T}{\Delta z} + \gamma_d \right)_2} \quad (6)$$



### 3.1. The water vapor problem.

The water vapor radiation problem was approached using a method presented by D. L. Brooks  $\overline{[1]}$  and based upon an adaptation of the flux divergence equation of Bruinenberg:

$$\left(\frac{\partial T}{\partial t}\right)_{wv} = \frac{q}{c_p} \left(\frac{p}{1000}\right)^{1/2} \left[ \sum_{n=1}^N \Delta(\sigma T^4)_n \left(\frac{\partial \overline{\epsilon}_s}{\partial w}\right)_n - \left(\sigma T^4 \frac{\partial \overline{\epsilon}_s}{\partial w}\right) - \sum_{m=1}^M \Delta(\sigma T^4)_m \left(\frac{\partial \overline{\epsilon}_s}{\partial w}\right)_m \right] \quad (7)$$

where  $q$  is the specific humidity at the reference level at which  $\frac{\partial T}{\partial t}$  is to be computed;  $\left(\frac{p}{1000}\right)^{1/2}$  is the Elsasser pressure correction factor; and  $\Delta(\sigma T^4)$  is the change in the Stefan-Boltzmann black body flux between successive levels of temperature  $T$  in the sounding. The summation index  $n$  denotes successively higher levels in the atmosphere above the reference level and the index  $m$  the layers below the reference level. The partial derivative  $\frac{\partial \overline{\epsilon}_s}{\partial w}$  is the slope of the curve of emissivity of water vapor, plotted against corrected optical depth and the term  $\sigma T^4 \frac{\partial \overline{\epsilon}_s}{\partial w}$  is evaluated at the top of the sounding.

The factors  $\frac{\partial \overline{\epsilon}_s}{\partial w}$  are evaluated as finite difference slopes from Brooks' curve<sup>1</sup>. In addition to the curve Brooks  $\overline{[1]}$  also presents tabular values of the mean slope of the emissivity curve for small increments of optical path-length.

If the convention in using eq. (7) is that  $\frac{\partial \overline{\epsilon}_s}{\partial w}$  is always positive when temperature decreases with height above the reference level, cooling

<sup>1</sup> Not shown here but presented in  $\overline{[1]}$ .



at the reference level results from the layer contributions above.

Similarly when the temperature from the ground decreases up to the reference level, the contributions from below yield warming at the reference level. The second term on the right, representing radiation divergence from the top of the sounding, gives a cooling contribution at the reference level. The actual conventions used in working with the tables are somewhat different, however, and were designed for maximum efficiency in machine computation.

In the application of the method, the initial step is the computation of the corrected optical depth,  $w$ , given by:

$$w = \frac{1}{g} \int_{p_0}^{p_1} \bar{q} \left( \frac{p}{p_s} \right)^{1/2} dp \quad (8)$$

where  $p_0$  and  $p_1$  are the layer boundary pressures and  $p_s$  is a standard pressure, 1000 mb.

Eq. (8) is approximated for a given layer by using mean values of  $q$  and  $p$ , and a finite pressure increment  $\Delta p$ :

$$\Delta w = -\bar{q} \frac{\Delta p}{980} \left( \frac{\bar{p}}{1000} \right)^{1/2} \quad (9)$$

When increments of optical path length,  $\Delta w$ , are calculated for each layer, values of  $\frac{\partial \bar{\epsilon}_s}{\partial w}$  may be obtained by interpolation in the table, using values  $w$  and  $w + \Delta w$  in entering the table.

When this work was begun the decision was made to perform the computations by hand methods rather than by electronic digital computer. This decision was in part based on the fact that use of the then available computer, the National Cash Register Company Model 102A, would have



necessitated lengthy computation times exclusive of the time required for programming. This observation is based on the fact that there are over 1000 entries in Brooks' table and only about as many storage cells in the computer. If the 102A had been used it would have been necessary to store the entire table on magnetic tape, which would virtually have eliminated the computation time-advantage of the computer. This difficulty may now have been overcome with the advent of the Control Data Corporation model 1604 computer. The larger storage capacity (over 32,000 cells) and extremely high speed of this new computer would lend itself well to Brooks' tabular method.





### 3.2. The carbon dioxide radiation problem.

For the carbon dioxide part of the radiation problem it was decided to employ a simple set of working equations previously used by Brooks [2] in stratospheric investigations of carbon dioxide radiative transfer.

The downward flux of infrared radiation at a level in the atmosphere and for a given frequency band (12.2 - 17.5  $\mu$  for CO<sub>2</sub>) is given by the Schwarzschild equation integrated over all angles:

$$F \downarrow (w_1) = F \downarrow (0) \tau_F (0, w_1) + \sum_{i=1}^n \bar{B}_i \Delta \tau_{Fi} \quad (10)$$

where  $F \downarrow (w_1)$  is the downward flux of diffuse radiation at the reference level, where  $w = w_1$ ;  $w_1$  is the optical path length of CO<sub>2</sub> above the level;  $F \downarrow (0)$  is the flux down from the top of the atmosphere;  $\tau_{Fi} (0, w_1)$  is the transmissivity of diffuse radiation by a slab of optical path  $w_1$ ; and  $\bar{B}_i = .185 \sigma T^4$  is the total black body flux<sup>1</sup> radiated by CO<sub>2</sub> at the appropriate mean temperature of the  $i^{\text{th}}$  layer.

The summation index  $i$  runs through  $n$  layers from the top of the atmosphere to the level in question.  $\Delta \tau_{Fi}$  is the increment to the flux transmissivity at the level  $w_1$  contributed by each layer.

Similarly the upward flux  $F \uparrow (w_1)$  is:

$$F \uparrow (w_1) = F \uparrow (w_0) \tau_F (w_1, w_0) + \sum_{j=1}^m \bar{B}_j \Delta \tau_{Fj} \quad (10)$$

where  $F \uparrow (w_0)$  is the upward flux at the ground; and  $\tau_F (w_1, w_0)$  is the transmissivity (assumed independent of temperature) of the slab of

<sup>1</sup> A carbon dioxide contribution equal to 18.5% of the black body radiation is quoted by various authors.



optical thickness  $w_0 - w_1$ , or from the ground to the reference level. The summation  $j=1$  through  $m$  runs from the ground to the level  $w_1$ .

In using these equations it is assumed that each layer can be approximated by an isothermal layer whose absolute temperature is the actual mean fourth root of the temperature of the layer raised to the 4th power. Since the soundings do not run to the top of the atmosphere,  $F \downarrow (0)$  was computed at the top of each sounding.

The net flux at the reference level ( $w_1$ ) is then simply:

$$F_N(w_1) = \bar{F}\uparrow(w_1) - \bar{F}\downarrow(w_1) \quad (12)$$

and the flux divergence,  $\Delta F_N$ , is taken as being the difference of net flux at two adjacent levels, the assumption being that the net flux divergence is uniform between the two layers. The hourly-temperature change in terms of the flux divergence in the layer is then:

$$\left(\frac{\partial T}{\partial t}\right)_{CO_2} = 4.1 \times 60 \times \frac{\Delta F_N}{\Delta p} \quad (13)$$

where flux is in  $\text{cal/cm}^2/\text{min}$  and pressure is in millibars.

For the determination of flux-transmissivity  $\tau_F$ , several choices were available as to method. Callender  $\overline{[4]}$  gives formulas for  $\tau_F$  based on a breakdown of the 12.5 - 17.5  $\mu$  band into five smaller wave length intervals. Burch and Howard  $\overline{[3]}$ , and Howard, Burch and Williams  $\overline{[8]}$  give two empirical formulas based on laboratory data for the total absorption of the 12.2 - 17.5  $\mu$  band:

"Strong" fit:  $\int A_\nu d\nu = -68 + 55 \log w + 47 \log (p + \beta) \quad (14)$

"Weak" fit:  $\int A_\nu d\nu = 3.16 w^{1/2} (p + \beta)^{.44} \quad (15)$



It follows then that  $\bar{A} = \frac{\int A_{\nu} d\nu}{\int d\nu} = \frac{\int A_{\nu} d\nu}{250 \text{ c.m.}^{-1}}$

and  $\tau_{\text{E}} = 1 - \bar{A}$

In (14), (15)  $w$  is absorber concentration in atmosphere-centimeters;  $p$  is atmospheric pressure in mm Hg; and  $\beta$  is the partial pressure of  $\text{CO}_2$  (assuming a constant ratio by weight, .00046, of the atmosphere.)

The Howard et al expressions (14) are for the "strong" fit or relatively large values of  $w$  and (15) for "weak" fit or relatively small values of  $w$ . The cut-off value given is 20% absorption, the log expression applying for  $A > 20\%$  and the exponential expression applying for  $< 20\%$ .

Both of the methods discussed above have the disadvantage of extremely lengthy computation-time for the data under consideration unless an electronic digital computer is used. Furthermore, the empirical equation of Howard et al has the disadvantage of a discontinuity between the two equations near absorptivities of 20%. A third and faster choice presented itself in the form of a curve giving fractional absorption  $\bar{A}$  vs pressure x path length (mb-cm-atmos) given by Brooks  $\langle \bar{2} \rangle$ , and credited by Brooks to Burch and Howard  $\langle \bar{3} \rangle$  (see fig. 2.) This curve had the advantage of affording greater facility in conjunction with hand computations, and it had no obvious discontinuities. A difficulty presented itself, however, after the  $\text{CO}_2$  computations were well underway when it was discovered that use of the Brooks curve yielded positive  $\text{CO}_2$  radiative flux divergences near the ground where large negative water-vapor flux divergences were obtained. Since this occurred near the level where absorptivities of 20% might be expected, the difficulty was overcome by



changing from the curve to the Howard et al "weak" fit expression for curve absorptivities less than 20%.

Although Brooks credits the curve to Burch and Howard  $\overline{3}$ , it is not entirely clear how he obtained his curve. The Burch and Howard curve is similar to that of Brooks except that their ordinate is percent transmission and the abscissa parameter is absorber concentration (cm-atmos). The Burch and Howard curve was obtained from data based on the use of the two empirical formulas, the discontinuity being smoothed out in the construction of the curve. Thus, regardless of how the smoothing was done in obtaining Brooks' curve it is clear that it is based on the empirical expressions of Burch and Howard. On this basis, changing from the curve, fig. 2, to the "weak" fit formula where necessary is justified, the discontinuity being accepted.

For the sake of comparison, values of percent absorption due to the "weak" fit formula are plotted in fig. 2 along with Brooks' curve. In the latter, a value of the "strong" fit formula corresponding to an curve absorption of 20% is shown. It appears that the smoothing in the region of 10-20% absorption favored the "strong" fit curve.

Since the fractional concentration of  $\text{CO}_2$  by weight in the atmosphere is nearly constant with height, the amount near any pressure level over a given vertical distance may be expressed in terms of a pressure difference. Thus every 4.2 mb of atmospheric air is equivalent to 1 cm-atmos of carbon dioxide (ie, a layer of  $\text{CO}_2$  of thickness 1 cm if reduced to S.T.P.). Taking the diffuse radiation through a slab to be





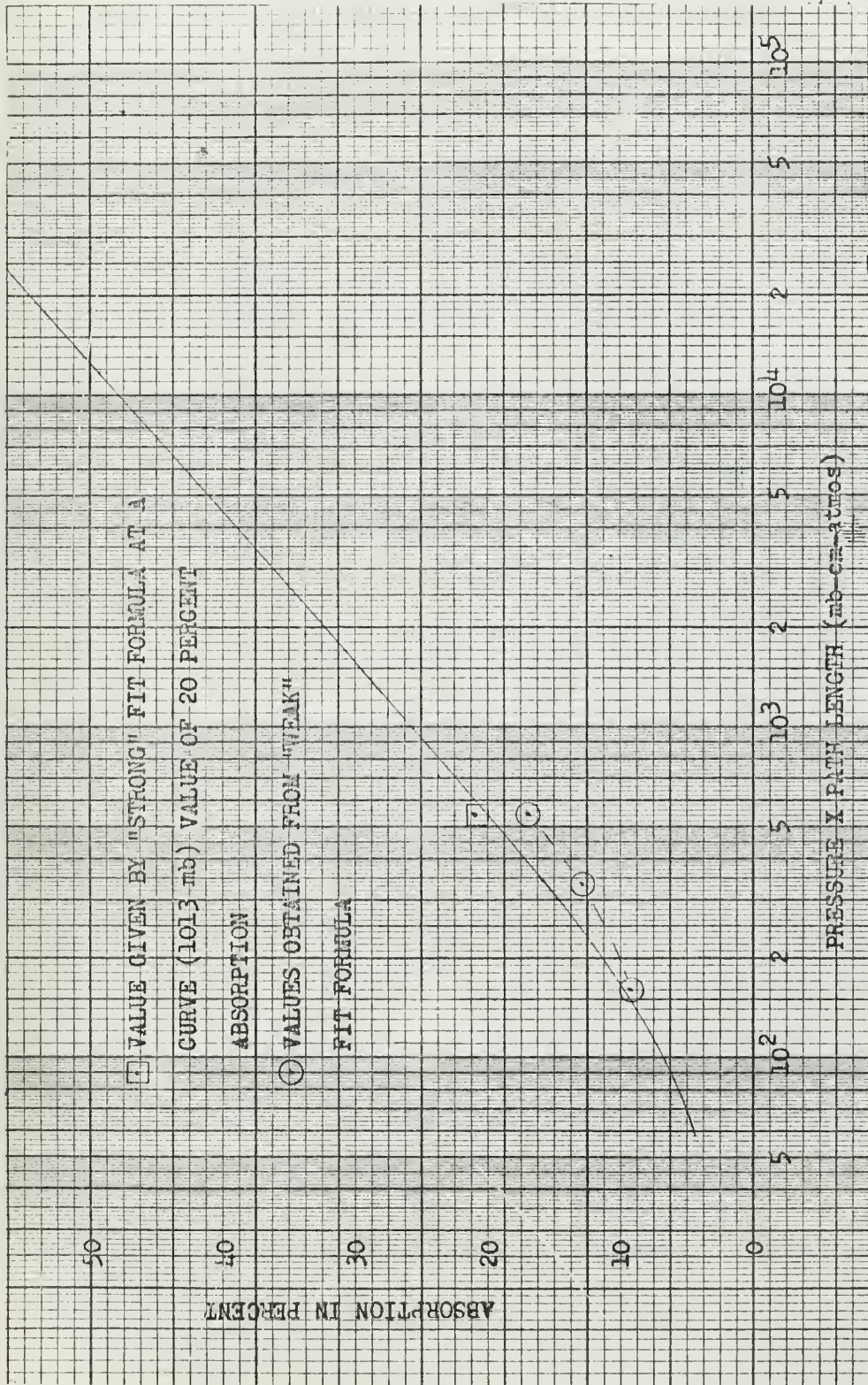


Fig. 2. Percent absorption of terrestrial radiation due to CO<sub>2</sub> in the 12.2-17.5<sub>μ</sub> band (after Brooks)



1.67 times that through a parallel radiating column, the equivalent optical path is:

$$W = \frac{1.67}{4.24} \int_{p_1}^{p_2} dp = .394 \Delta p \text{ (cm-ATMOS)} \quad (16)$$

This is the absorber-concentration in the Burch and Howard expression.

For use with Brooks' curve,  $w$  is linearly pressure-weighted giving  $w'$  as follows:

$$W' = \frac{1.67}{4.24} \int_{p_1}^{p_2} p dp = .394 \bar{p} \Delta p \quad (17)$$

with  $w'$  now in mb-cm-atmos and  $\bar{p}$  the mean pressure of the layer.



#### 4. Computations.

##### 4.1. The water vapor radiative temperature change.

The radiative temperature changes due to water vapor were computed by use of the method discussed in section 3.1. Required are the knowledge of temperature, pressure, pressure differences, and relative humidity at the given reference levels, the reference levels being taken as 8, 17, 35, 100, 165, and 240 meters. Here, conditions at 16.0 meters are assumed to apply at 17 meters, so that in some cases, in order to smooth out artificial inversions in the temperature data between 16.0 and 17 meters, it was necessary to shift the MIT temperatures so that the 16.0 meter MIT temperature would correspond to the 17 meter L-20 temperature.

The pressure, and layer pressure differences were computed by use of the hypsometric equation together with the known temperature profile. Values of specific humidity were obtained from the aerograph humidity data, radiosonde data, and station humidity. Unfortunately instrumental failure left a hole in the micrometeorological humidity data between the station values and the aerograph soundings. For levels between station values and aerograph soundings, linear interpolation with height was assumed valid in arriving at values of  $\bar{q}$  for the reference levels. As noted, radiosonde data was used to extend the data above the maximum level of L-20 flight. This was done by "hooking" on to the nearest radiosonde reporting level after the highest reported L-20 data were exhausted.



The computed water vapor radiative temperature changes are given in table 1. Note the strong radiative warming tendency in the lower layers at midday, tending to change to cooling in the neighborhood of 100 m. This effect has already been noted by Cooley [5].

Table 1. Infrared radiative temperature change ( $^{\circ}\text{C}/\text{Hr.}$ ) due to water vapor (times in CST).

Reference level (meters)	Times					
	0635	0835	1035	1235	1435	1635
8	-0.13	1.25	2.00	3.05	2.23	0.71
17	-0.07	0.12	0.17	1.87	0.92	0.10
35	-0.02	0.14	0.20	0.13	0.50	-0.07
51	-0.09	0.09	0.07	-0.11	0.10	-0.14
100	-0.14	0.03	0.02	0.22	-0.01	-0.08
165	-0.19	0.09	-0.03	0	-0.01	-0.01
240	-0.17	-0.20	-0.05	-0.03	-0.06	-0.05





4.2. The radiative temperature change due to carbon dioxide.

The CO<sub>2</sub> radiative temperature changes were computed by the method of section 3.2 and are shown in table 2. Since the mean black body flux  $\overline{\sigma T^4}$  for layers was needed in the CO<sub>2</sub> method, plots of  $\sigma T^4$  versus height were made for the layers from 0 to 16 meters, and  $0.185 \times \overline{\sigma T^4}$  approximated by equal-area averaging. Above 16 meters,  $0.185 \sigma T^4$  was simply averaged between levels.

Since the method yields  $(\partial T / \partial t)_{CO_2}$  in layers between reference levels, reference-level values were interpolated. On the average, CO<sub>2</sub> radiative temperature changes were found to be approximately 23% of the water vapor radiative changes, a result which also confirms that of Cooley [5] in these layers. Note also the tendency for the radiative temperature change to change sign near 240 meters in a manner similar to that of water vapor.

Table 2. Infrared radiative temperature change due to carbon dioxide (°C/Hr.)

Reference level (meters)	Times					
	0635	0835	1035	1235	1435	1635
8	-0.10	0.17	0.26	0.49	0.31	0.13
17	-0.02	0.06	0.15	0.26	0.25	0.08
35	0	0.03	0.07	0.09	0.10	0.01
51	0	0.02	0.05	0.06	0.06	0
100	0	0.02	0.02	0.02	0.02	0
165	0	0.01	0.01	0.01	0.02	0.01
240	-0.06	0	0.01	0	-0.01	0



#### 4.3. The local rate of change of temperature.

The local rate of change of temperature was obtained from the MIT data at 4.0, 8.0, and 16.0 meters and from the aerograph temperature data at 35, 51, 100, 165, and 240 meters. Since the observation times were centered bi-hourly at 35 minutes after the even hour,  $\frac{\partial T}{\partial t}$  was taken over a two hour period and centered at a time 35 minutes after the odd hour. For example, the local change from 0635-0835 CST was centered at 0735 CST. The aerograph temperature changes were obtained in a like fashion except that some difficulty was encountered in the use of this data. A plot of L-20 data with height yields two curves since data is taken on both ascent and descent of the aircraft. As an illustration, fig. 3 gives the L-20 temperatures for the 1235 sounding. Where data for the given reference level were missing smooth-curve interpolation was used. This would give an estimated  $\frac{\partial T}{\partial t}$  for a two-hour period either from the ascent or descent curves or both. Where doubt existed as to the representative values of  $\frac{\partial T}{\partial t}$  (i.e. whether to use the ascent or descent curves), either an average value from both ascent and descent curves, or a subjective choice of the most reasonable sounding was used. Since all periods were taken as two hour periods, an error in  $\frac{\partial T}{\partial t}$  may possibly exist due to a displacement in time away from the supposed observation times. This type of error is estimated to be no more than 5% however, and should be random in nature. Table 3 presents the observed (or estimated) values of  $\frac{\partial T}{\partial t}$ .



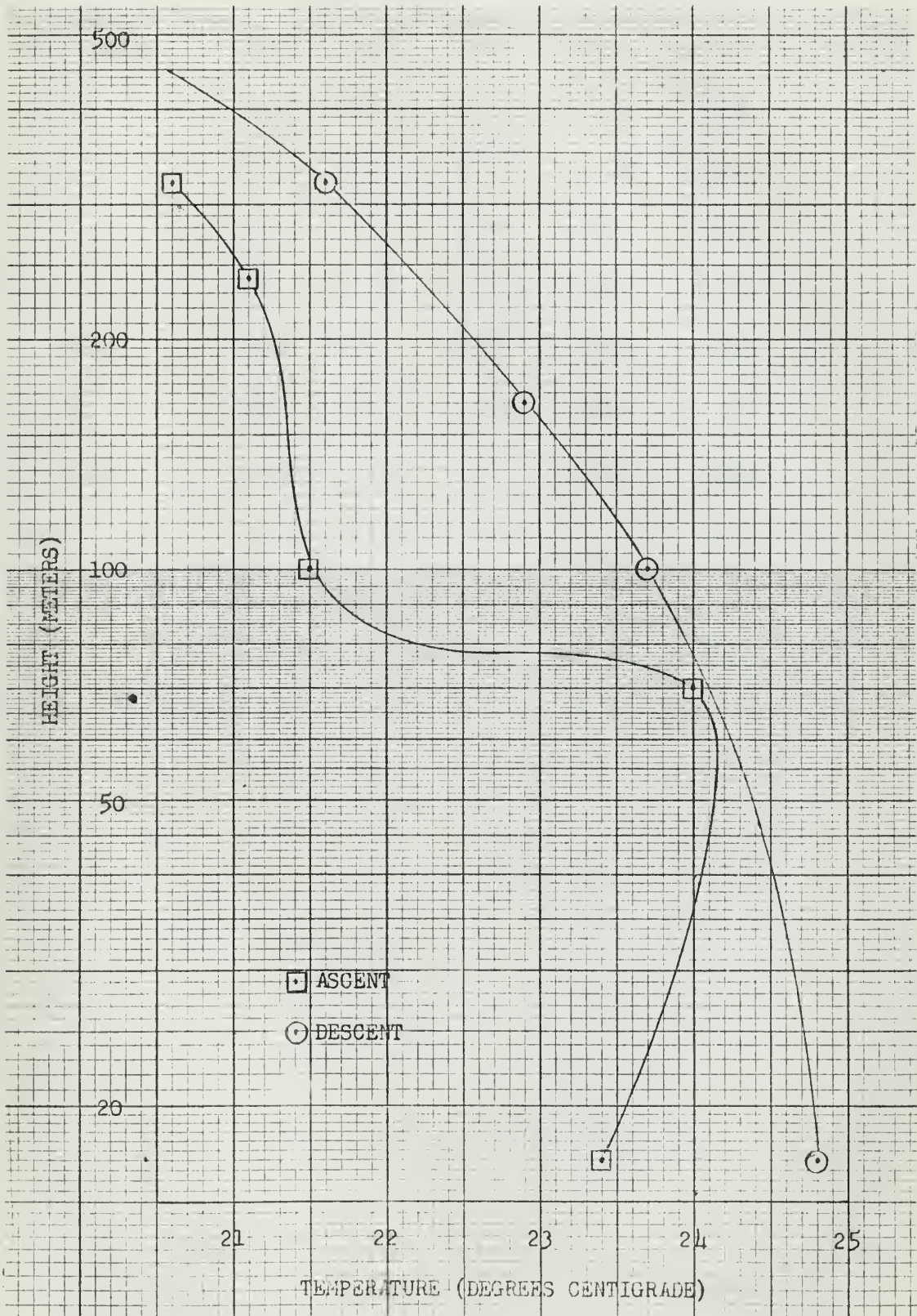


Fig. 3. L-20 aerograph temperature sounding at 1235 CST.



Table 3. Average local rate of change of temperature ( $^{\circ}\text{C}/\text{Hr}$ )

Reference level (meters)	Times				
	0735	0935	1135	1335	1535
8	3.24	2.27	1.61	1.07	0.12
17	2.98	2.23	1.55	1.14	0.15
35	2.08	2.67	1.41	0.80	0.45
51	1.58	2.68	1.49	0.67	0.35
100	0.61	2.61	0.87	0.80	0.40
165	-0.20	2.15	0.93	0.90	0.37
240	0.15	1.42	1.05	0.97	0.33





#### 4.4. Advective temperature changes.

Generally speaking, in computing  $K_H$  the assumption will be made that advection is zero. However, it may be shown from the quoted geostrophic winds  $\overline{\langle 10 \rangle}$  that this assumption is not quite valid for the period in question. Haltiner and Martin  $\overline{\langle 7 \rangle}$  have shown that the layer mean geostrophic advection is given by:

$$-\overline{V}_g \cdot \nabla_p \overline{T}_v = \frac{2-f}{Rd} \Delta A \ln \frac{p_1}{p_2} \quad (18)$$

where  $\overline{V}_g$  is the layer mean geostrophic wind;  $\overline{T}_v$  is the layer mean virtual temperature; and  $\Delta A$  is the cross-hatched area of the geostrophic wind hodograph in fig. 4.

Now computing the geostrophic mean advection for the layer 950-900 mb for 0900 CST on 7 September we get  $0.24^\circ\text{C}/\text{Hr}$ . Since the actual wind component perpendicular to the mean isotherms is about 17% of the mean geostrophic, the advection term of  $0.24^\circ\text{C}/\text{Hr}$  will be reduced to  $0.041^\circ\text{C}/\text{Hr}$ . Since the wind speeds increase in the afternoon it is probable that a somewhat larger advection will take place at this time. Unfortunately no other useful geostrophic components are given in the data other than for 0900. This consideration of advection, therefore, requiring more extensive investigation will not be pursued further in this paper<sup>1</sup>.

<sup>1</sup> Except for the 0935 sounding where the advection computed for 0900 will be used in the determination of a  $K_H$ , for comparison with a  $K_H$  computed without the advection consideration.



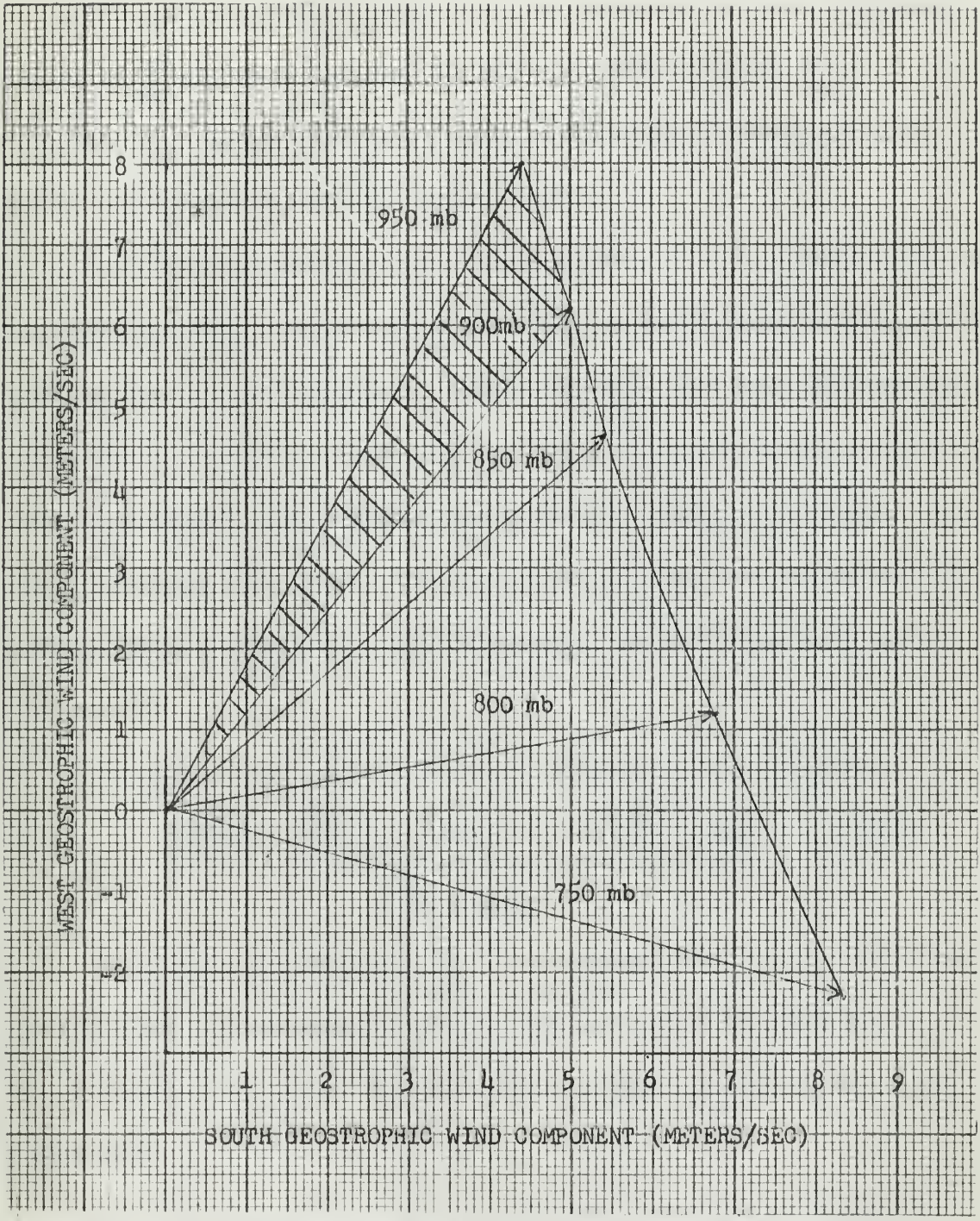


Fig. 4. Hodograph of the geostrophic wind for 7 September-0900 (values are estimated for the O'Neill site from local synoptic charts.)



4.5. The coefficient of eddy conductivity.

Having computed  $\left(\frac{\Delta T}{\Delta t}\right)_{RAD}$  it will be necessary to obtain  $\left(\frac{\Delta T}{\Delta z} + \gamma_d\right)$ . Values of  $\left(\frac{\Delta T}{\Delta z} + \gamma_d\right)$  were obtained by adding  $0.0098^\circ\text{C}/\text{m}$  to  $\frac{\Delta T}{\Delta z}$ .

To obtain  $\frac{\Delta T}{\Delta z}$  above 17 meters, plots of aerograph temperature with height were made on semi-log paper (see fig. 3).

Similarly for values up to 17 meters, plots of MIT micrometeorological temperatures with heights were made on linear graph paper and a smooth curve drawn through the points. Values of  $\frac{\Delta T}{\Delta z}$  were then obtained from the applicable curve by measuring the slope of the chord centered on the level in question. For vertical gradients at 17 meters<sup>1</sup> and below, one meter intervals were taken. For the levels 35 meters to 165 meters, 10-meter intervals were used, while 20-meter intervals were used above 165 meters.

Returning to eq. (6) and omitting advection, one obtains:

$$K_2 = \frac{\left[\left(\frac{\Delta T}{\Delta t}\right) - \left(\frac{\Delta T}{\Delta t}\right)_{RAD}\right] \Delta z_{i-2} + K_1 \left(\frac{\Delta T}{\Delta z} + \gamma_d\right)_1}{\left(\frac{\Delta T}{\Delta z} + \gamma_d\right)_2} \quad (20)$$

Because of the fact that  $\frac{\Delta T}{\Delta t}$  was centered after the odd hours and the radiative temperature change was centered after the even hours, it was decided to compute a  $\bar{K}_H$  centered after the odd hour by doing the following:

- (1) Averaging  $\left(\frac{\Delta T}{\Delta t}\right)_{RAD}$  for two adjacent after "the even hour" soundings, giving a  $\left(\frac{\Delta T}{\Delta t}\right)_{RAD}$  centered after "the odd hour".

<sup>1</sup>•The 16 meter change was assumed to apply at 17 meters.



(2) Repeat step (1) again for  $\frac{\Delta T}{\Delta z} + \gamma_d$  to obtain  $\overline{\left(\frac{\Delta T}{\Delta z} + \gamma_d\right)}$ , values of which are listed in table 4.

The previous steps yield the final recursion formula

$$\bar{K}_2 = \frac{\left[ \frac{\Delta T}{\Delta t} - \left(\frac{\Delta T}{\Delta t}\right)_{RAD} \right] \Delta z_{1,2} + \bar{K}_1 \overline{\left(\frac{\Delta T}{\Delta z} + \gamma_d\right)}_1}{\left(\frac{\Delta T}{\Delta z} + \gamma_d\right)_2} \quad (21)$$

where  $\bar{K}_1, \bar{K}_2$  are also centered after "the odd hours".

Table 4. Average lapse rate of potential temperature, ( $^{\circ}\text{C}/\text{meter}$ ).

Reference levels (meters)	Time				
	0735	0935	1135	1335	1535
4	0.0088	-0.1011	-0.1301	-0.1292	-0.0992
8	0.0173	-0.0277	-0.0402	-0.0482	-0.0287
17	0.0218	-0.0132	-0.0252	-0.0202	-0.0082
35	0.0138	-0.0137	-0.0047	0.0072	-0.0082
51	0.0183	-0.0057	-0.0042	-0.0052	-0.0062
100	0.0178	0.0023	-0.0042	-0.0032	-0.0042
165	0.0208	0.0073	-0.0027	0.0008	0.0003
240	0.0270	0.0143	0.0014	0.0003	0.0018

As an illustration of the form of this equation for obtaining  $\bar{K}_H$  at 17 meters,  $\bar{K}_{17}$ , the equation is:

$$\bar{K}_{17} = \frac{\left[ \left(\frac{\Delta T}{\Delta t}\right)_{OBS,8} - \left(\frac{\Delta T}{\Delta t}\right)_{RAD,8} \right] \Delta z_{4-17} + \bar{K}_4 \overline{\left(\frac{\Delta T}{\Delta z} + \gamma_d\right)}_4}{\left(\frac{\Delta T}{\Delta z} + \gamma_d\right)_{17}} \quad (21)$$

with  $\Delta z = 17 \text{ meters} - 4 \text{ meters} = 13 \text{ meters}$ .





Now a starting value of  $\bar{K}_H$  at four meters, with temperature changes at eight meters, yields a value of  $\bar{K}_H$  at 17 meters. Next to obtain the 35-meter  $\bar{K}_H$ , a starting value of  $\bar{K}_H$  at eight meters with temperature changes at 17 meters, is required. After this the computed value of  $\bar{K}_H$  at 17 meters is used to get a value at 51 meters, and the scheme is continued in leapfrog fashion until all values have been obtained.

As previously noted in section 1, table 5.a of  $\overline{\langle 10 \rangle}$  gives values of  $Q$  ( $\text{mcal cm}^{-2} \text{min}^{-1}$ ). These values were obtained from the correlation of rapid fluctuations of temperature and vertical motion using one-second samplings of fast response probes together with the Reynold's formula:

$$Q = -\rho C_p \overline{w' T'}$$

As a general principle, following Priestly  $\overline{\langle 11 \rangle}$ , the turbulent flux of heat may be considered constant with elevation in shallow layers above about one meter. The reported values, table 5.a of  $\overline{\langle 10 \rangle}$ , seem to substantiate this result up to 12 meters. Now values of  $Q$  given in table 5.2a of  $\overline{\langle 10 \rangle}$  are for 3.0, 6.0 and 12.0 meters. Averaging these to get representative values of  $Q$  in the layer 3 - 12 meters gives starting values of  $K_{H,4}$  and  $K_{H,3}$  obtained by using eq. (1).

One further complication exists, however, in the 1235 and 1435 soundings for which no MIT values of  $Q$  are given. Here it was decided to estimate values of  $Q$  from a comparison of the MIT values of  $Q$  and theoretical model values of  $Q_0$  at the earth-air interface. Two such theoretical models<sup>1</sup> were available with values for the 1235 and 1435

<sup>1</sup>. For a discussion of these theoretical models see Chapter 7.3 of  $\overline{\langle 10 \rangle}$ .



reports ; one due to Suomi  $\overline{Q_0}$  and one due to Lettau  $\overline{Q_0}$ .

Considering the entire seventh observation period, Lettau's values of  $Q_0$  were found to correlate more highly with the reported values of turbulent heat transfer  $Q$  than did the  $Q_0$  values of Suomi. On this basis, a ratio of the average observed  $Q$  to the Lettau theoretical value  $Q_0$  for the 1035, 1235, and 1435 observations for all observation periods at O'Neill, Nebraska was calculated. 1035 values were included to give enough values on which to base this ratio. The ratio was then applied to the  $Q_0$  of the Lettau theory for 1235 and 1435 so that  $Q_4$  and  $Q_8$  for these times could be obtained. Computed values of  $\overline{K_H}$  are given in table 5.



Table 5. Computed values of  $\bar{K}_H$ , (cm<sup>2</sup>/sec.)

Reference level (meters)	Time s				
	0735	0935	0935*	1135	1335
4	3,720	5,764	5,764	4,870	5,020
8	10,620	19,450	19,450	16,050	13,300
17	5,875	43,000	43,055	26,960	35,550
35	29,350	28,480	28,711	132,000	94,400
51	17,330	58,750	59,794	135,000	131,100
100	38,600	30,750	27,536	85,000	177,700
165	25,300	66,600	63,928	116,000	2,340,000
240	23,200	62,500	61,889	5,500	-744,000
320	45,400	99,100	95,906	86,200	-20,800
					-1,394,000
					-247,000
					-181,000

\*The column identified by the symbol \* includes the advective rate of change of temperature in the computation of  $\bar{K}_H$ .



5. Results.

5.1.  $\bar{K}_H$  as a function of height.

Considering the values of  $\bar{K}_H$  given in table 5 up to the point where there is a sharp drop off in values with respect to height<sup>1</sup>, the computed values of  $\bar{K}_H$  show a strong linear trend when plotted on log-log paper.

To substantiate this linear trend, correlation coefficients of log  $\bar{K}_H$  and log  $Z$  were computed and regression lines of best fit were obtained and plotted for the data for each sounding (see figs. 5-10).

Now a straight line plot of  $K_H$  with  $Z$  on log-log paper yields  $\bar{K}_H$  as a function of exponential height according to the general equation:

$$\frac{K_H}{K_1} = \left(\frac{Z}{Z_1}\right)^m \quad (22)$$

Computed equations for  $\bar{K}_H$  as an exponential function of height are presented in table 6.

Table 6.  $K_H$  as an exponential function of height.

Time (CST)	Equation	Range of Heights on which the equation is based (meters)
0735	$\bar{K}_H = 2690 Z^{.478}$	4 - 320
0935	$\bar{K}_H = 5653 Z^{.480}$	4 - 320
0935 <sup>2</sup>	$\bar{K}_H = 5799 Z^{.468}$	4 - 320
1135	$\bar{K}_H = 2601 Z^{.854}$	4 - 165
1335	$\bar{K}_H = 294.8 Z^{1.428}$	4 - 165
1535	$\bar{K}_H = 1500 Z^{1.003}$	4 - 100

<sup>1</sup>Negative values, and values above 165 meters for the 1135 sounding, were excluded.

<sup>2</sup>Advection neglected in the computations except for the second result at 0935, for which the 0900 computed advection was assumed to apply at 0935.

RESULTS

Conversion of the various  $\bar{M}_w$  values to table 3 up to the level where  $\bar{M}_w$  drops sharply or to 1000 with respect to  $\bar{M}_w$ . The computed values of  $\bar{M}_w$  from 3 to 1000 were then plotted on log-log paper to give the curves shown in Figure 1. The theoretical molecular weights of the  $\bar{M}_w$  and  $\bar{M}_n$  were computed and reported lines of best fit were obtained for the data for each condition (see Figs. 2-10).

From a plot of  $\log \bar{M}_w$  vs.  $\log \bar{M}_n$  with 3 on the log paper yields  $\bar{M}_w$  as a function of experimental number according to the general equation:

$$\bar{M}_w = K \bar{M}_n^x \quad (25)$$

General equations for  $\bar{M}_w$  as a function of experimental number are presented in table 4.

Table 4.  $\bar{M}_w$  as a function of experimental number.

Range of Heights on which the equation is based (meters)	Equation	Time (min)
2 - 300	$\bar{M}_w = 2.1 \bar{M}_n^{1.1}$	100
1 - 310	$\bar{M}_w = 2.1 \bar{M}_n^{1.1}$	100
4 - 310	$\bar{M}_w = 2.1 \bar{M}_n^{1.1}$	100
4 - 163	$\bar{M}_w = 2.1 \bar{M}_n^{1.1}$	100
2 - 167	$\bar{M}_w = 2.1 \bar{M}_n^{1.1}$	100
4 - 100	$\bar{M}_w = 2.1 \bar{M}_n^{1.1}$	100

These equations are based on the data for the 115 seconds run. The values of  $\bar{M}_w$  and  $\bar{M}_n$  are given in the text. The values of  $\bar{M}_w$  and  $\bar{M}_n$  are given in the text. The values of  $\bar{M}_w$  and  $\bar{M}_n$  are given in the text.



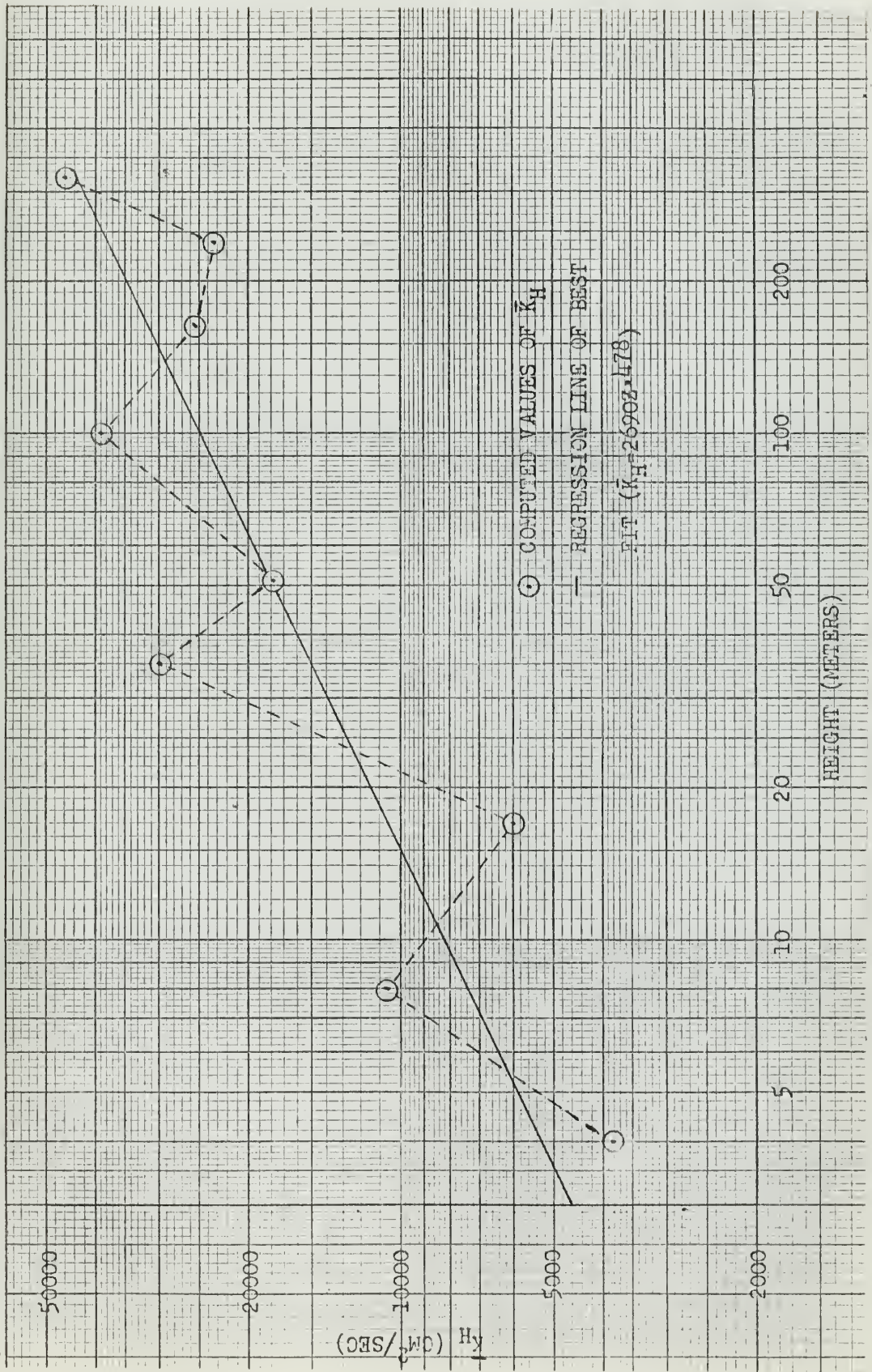


Fig. 5.  $\bar{K}_H$  as a function of height for the 0735 sounding.



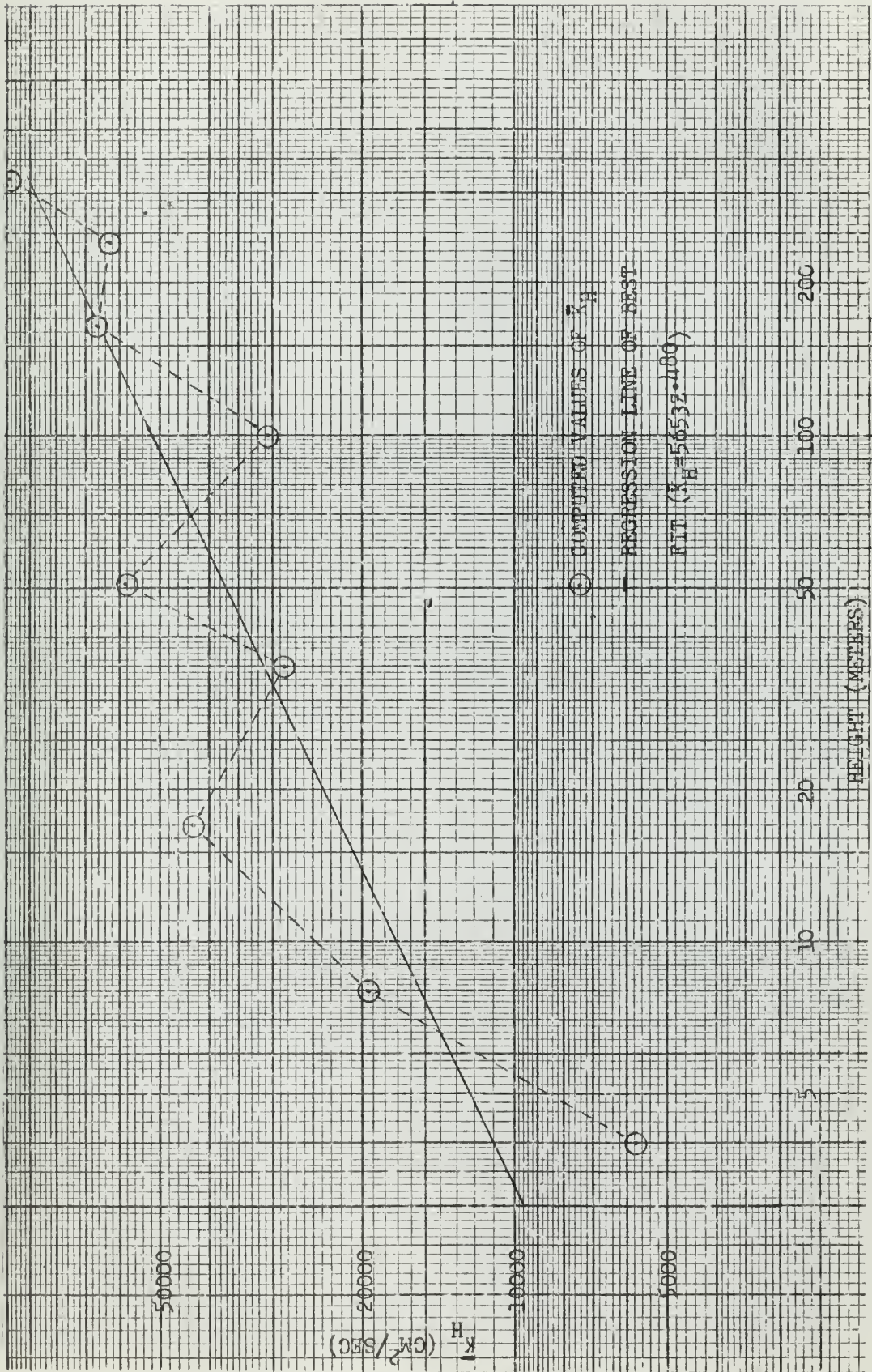


Fig. 6.  $\bar{K}_H$  as a function of height for the 0935 sounding (without advection.)



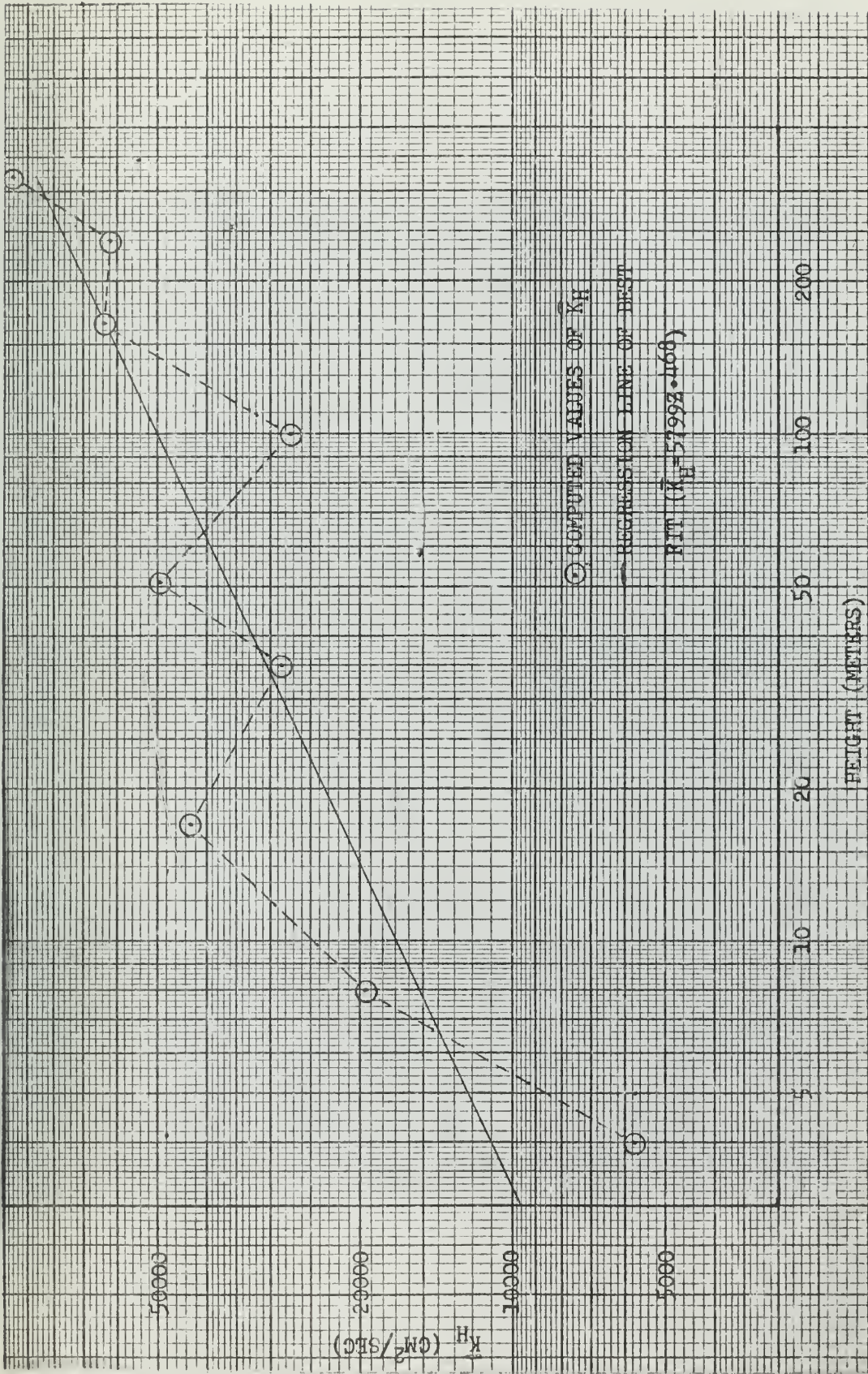


Fig 7.  $\bar{K}_H$  as a function of height for the 0935 sounding (with advection.)



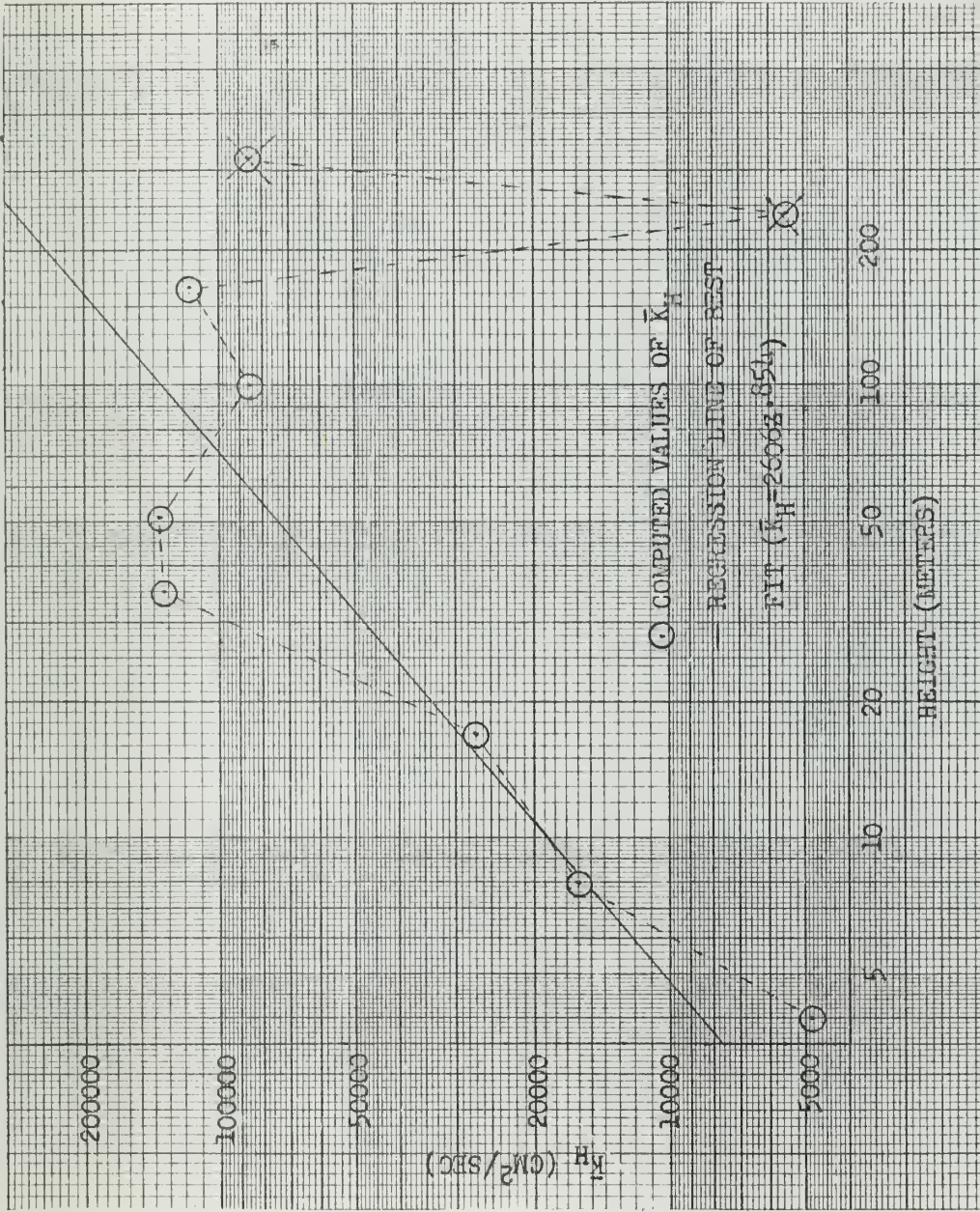


Fig. 8.  $\bar{K}_H$  as a function of height for the 1135 sounding.





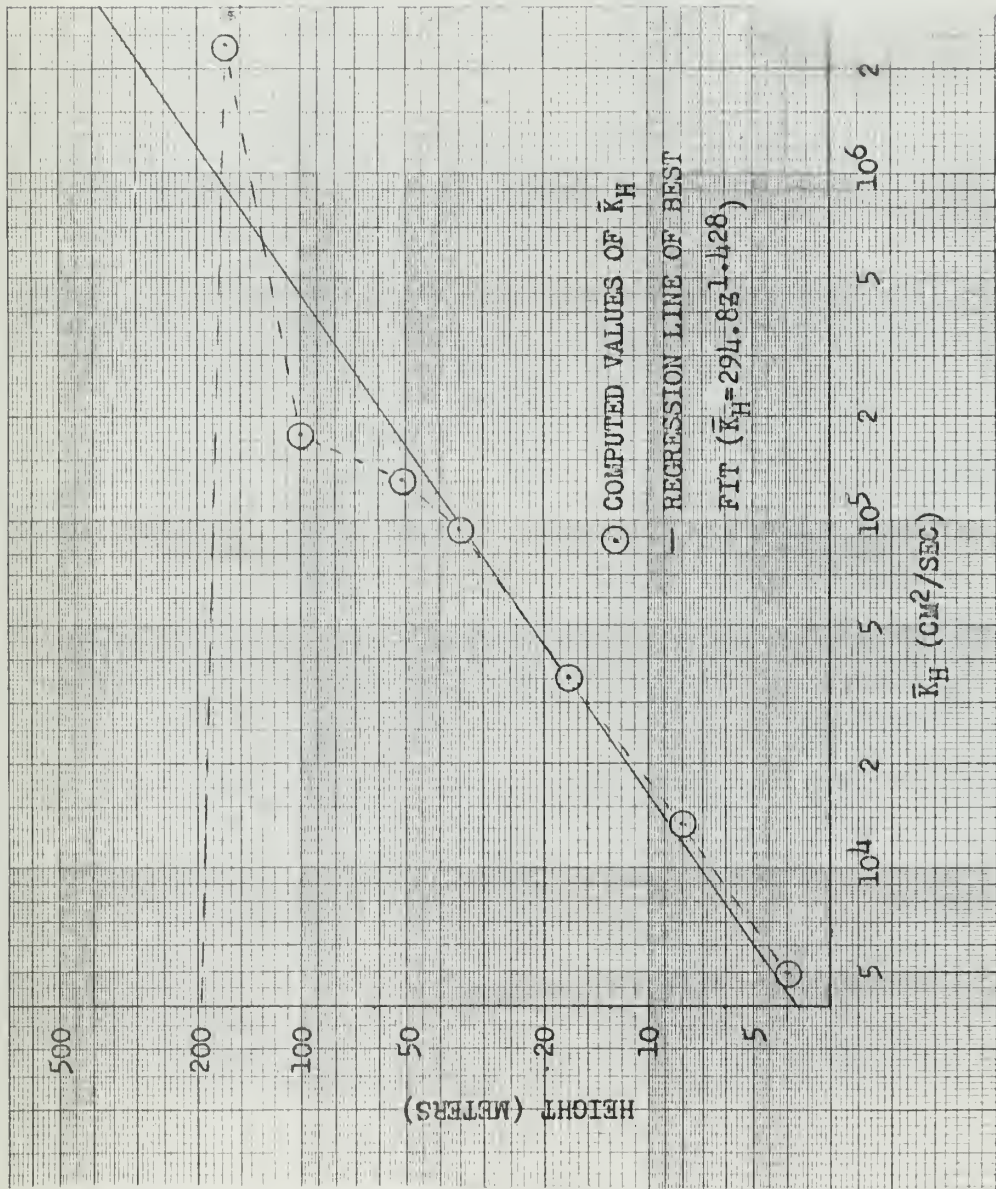


Fig. 9.  $\bar{K}_H$  as a function of height for the 1335 sounding.



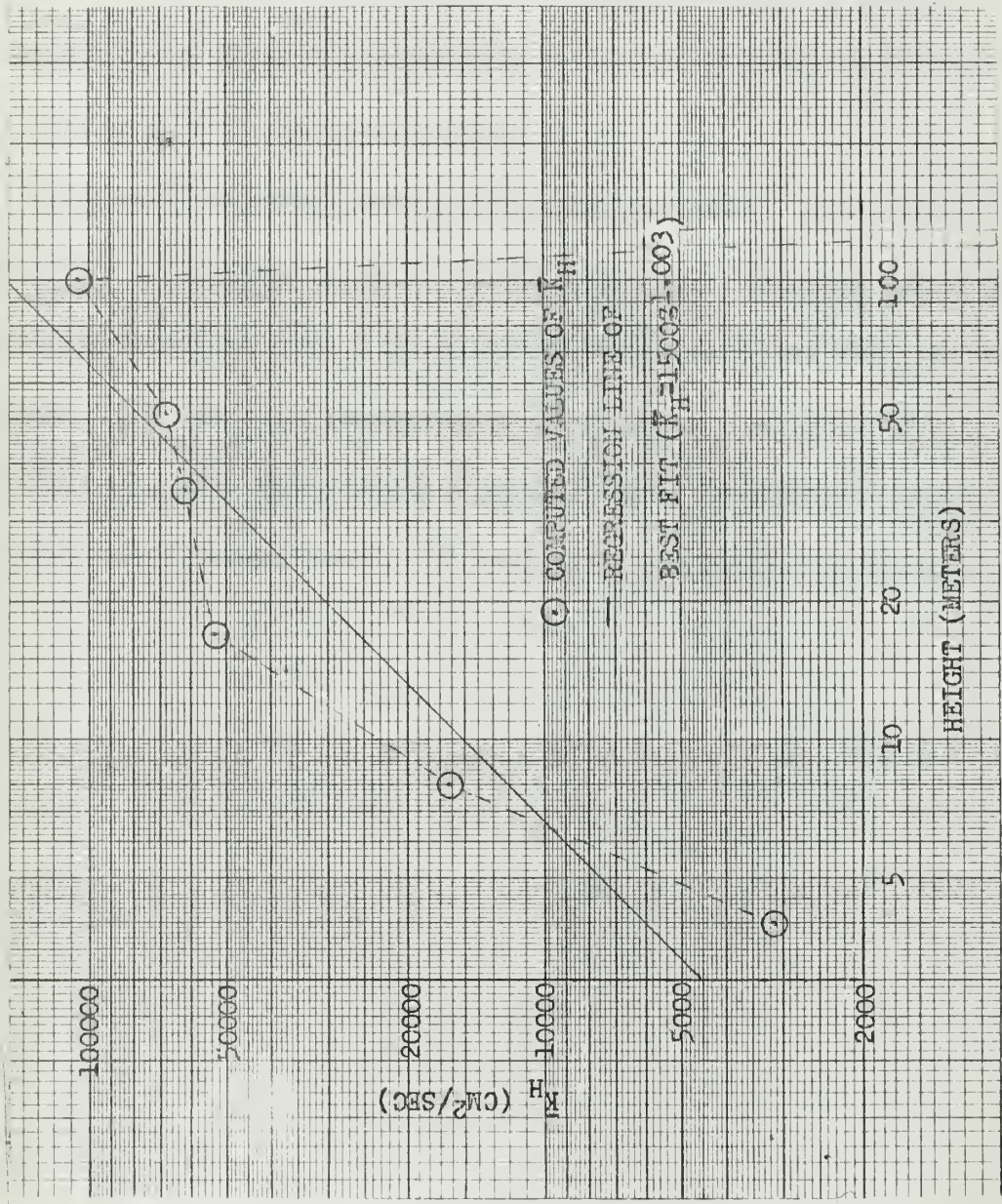


Fig. 10.  $\bar{K}_H$  as a function of height for the 1535 sounding.



- It is to be noted that where advection was considered (0935 case) the result was not greatly different from that in which this parameter was neglected. The difference, however, indicates that the  $\bar{K}_H$ - values, with advection included, were slightly greater in the lower portion of the layer, and smaller in the upper portion.

It should also be pointed out that in most cases, the values of  $\bar{K}_H$  computed for elevations above 165 meters showed a decrease below the value at the previous level. In several cases, the values of  $\bar{K}_H$  were negative. This was most likely due to observational errors in  $(\overline{\partial T / \partial z + \gamma_d})$ , when  $\partial T / \partial z$  was very close to the adiabatic lapse, a condition which occurred in the neighborhood of 165 meters for the midday and afternoon runs.



5.2.  $\bar{K}_H$  as a function of stability.

It would have been appropriate to compare values of  $\bar{K}_H$  and  $m$  to a stability parameter such as the Richardson number. Since appropriate wind data for such a comparison were not available, it was more feasible to correlate  $\bar{K}_H$  and  $m$  with a significant part of the numerator<sup>2</sup> of the integrated Richardson number,  $\Delta\Theta$ . This was done and the results are tabulated below.

Table 7. Linear correlation coefficients of  $\Delta\Theta$  with  $\bar{K}_H$  and  $\Delta\Theta$  with  $m$  at indicated heights.

$K_H^1$ (meters)	$\Delta\Theta$ computed over layers (meters)	Correlation coefficients of $\bar{K}_H$ with $\Delta\Theta$	Correlation coefficients of $m$ with $\Delta\Theta$
4	2-4	0.26	-0.73
8	2-8	-0.77	-0.71
17	2-17	-0.96	-0.68
35	2-35	-0.88	-0.84
51	2-51	-0.76	-0.75
100	2-100	-0.67	-0.75

Considering values of  $\Delta\Theta$  versus  $\bar{K}_H$  at heights from four to 100 meters for all soundings (sample size 30) a correlation coefficient of -0.43 is obtained.

<sup>1</sup>Values obtained from equations given in table 6.

<sup>2</sup>Here  $\Delta\Theta = \Theta(z) - \Theta(2)$

where  $z$  is variable and  $\Theta(2)$  is the value of  $\Theta$  at  $z = 2$  meters.





## 6. Conclusions.

Although negative values of  $\bar{K}_H$  are somewhat disconcerting, other investigators have been confronted with this anomaly at much lower levels [6]. As mentioned earlier, factors possibly contributing to these negative values are chiefly non-representative lapse rates due to errors in the measurement of temperature, especially as the lapse rate of temperature approaches the dry adiabatic. Still another possibility arises when one considers the theory of Priestly and Swinbank concerning forced versus free convection (see for example p. 261 of [7]).

From an inspection of the computed power-law profiles for  $\bar{K}_H$  listed in table 6, it appears that  $m$  increases inversely with stability, the maximum value of  $m$  occurring in the early afternoon. Although it is doubtful whether the correlations listed in table 6 can be proved statistically significant on the basis of such a small sample size (five), nevertheless it is felt that a strong physical significance is inherent in the repetitive nature of the results, and that  $\bar{K}_H$  has a strong inverse dependence on stability. This statement is given support by the results of a correlation of the  $\Delta\Theta$  parameter with all values of  $\bar{K}_H$  represented in table 7 (sample size 30) where a statistically significant<sup>1</sup> correlation coefficient of -0.43 is obtained. Further it is apparent, from an inspection of table 7 that this correlation (-0.43) could be further improved by the elimination from consideration of values of  $\bar{K}_H$  at four meters where a positive correlation of  $K_H$  with  $\Delta\Theta$  is obtained. Considering the positive correlation of  $K_H$ ,

<sup>1</sup>At the five percent level of belief.



with  $\Delta\Theta$  and the negative correlation of  $\bar{K}_{H,3}$  with  $\Delta\Theta$ , it seems likely that the method of computing  $\bar{K}_H$  at four and eight meters may have affected the overall correlation. It must be remembered that the assumption made in this connection was that  $Q_{TURB}$  is independent of elevation from one to 12 meters. At higher levels, the computational procedure gave considerably larger  $\bar{K}_H$ -values which then varied consistently (if not "significantly") with stability.

In summary, daytime-values of  $\bar{K}_H$  obtained under the conditions of the Great Plains Turbulence Field Program  $\langle \bar{10} \rangle$ , tend to increase with increasing lapse rate, and with increasing height up to at least 100 meters. Above some such level  $\bar{K}_H$  seems to decrease. It is possible that a specific function  $K_H = f(Ri)$  may exist, but the data was not sufficiently detailed to establish such a result at this time.



## BIBLIOGRAPHY

1. Brooks, D. L., A tabular method for the computation of temperature change by infrared radiation in the free atmosphere. *J. Meteor.*, 5, 313-321, 1950.
2. Brooks, D. L., The distribution of carbon dioxide cooling in the lower stratosphere. *J. Meteor.*, 2, 210-219, 1958.
3. Burch, D<sup>s</sup> and J. N. Howard, Infrared transmission of blackbody radiation through the atmosphere. AFCRS-TN-55-857, RF Project 535, Scientific Report 2, Geophys. Research Directorate, Air Force Cambridge Research Center, Cambridge, Mass., May 1955.
4. Callendar, G. S., Infrared absorption by carbon dioxide, with special reference to atmospheric radiation. *Quart. J. R. Meteor. Soc.*, 67, 263-275, 1941.
5. Cooley, B. C., Determination of the diurnal variation of eddy conductivity near the Earth's surface. U. S. Naval Postgraduate School Master's thesis, 47 pp, 1950.
6. Cramer, H. E. and F. A. Record, The variation with height of the vertical flux of heat and momentum. *J. Meteor.*, 3, 219-226, 1953.
7. Haltiner, G. J. and F. L. Martin, *Dynamical and Physical Meteorology*. Mc-Graw-Hill, New York, 470 pp, 1957.
8. Howard, J. N., D. Burch, D. Williams, Near-infrared transmission through synthetic atmospheres. *Geophys. Res. Pap.* 40, AFCRC-TR-55-213, Geophys. Research Directorate, Air Force Cambridge Research Center, Cambridge, Mass., Nov. 1955.
9. Jehn, K. H. and J. R. Gerhardt, A preliminary study of the eddy transfer of heat near the Earth's surface. *J. Meteor.*, 5, 343-346, 1950.
10. Lettau, H. and B. Davidson, *Exploring the Atmosphere's First Mile*. 2 vols., Pergamon Press, New York, 1957.
11. Priestly, C. H. B., *Turbulent Transfer in the Lower Atmosphere*. The Univ. of Chicago Press, Chicago, 1959.















thesC7564

A determination of the coefficient of ed



3 2768 002 08976 5

DUDLEY KNOX LIBRARY